Permissible Three-Dimensional Testing in a Two-Dimensional Adaptive Wall Wind Tunnel

David Sumner* and Ewart Brundrett†
University of Waterloo,
Waterloo, Ontario N2L 3G1, Canada

Introduction

RECENT low-speed experiments with disk models in a two-dimensional adaptive flexible wall test section[1] have supported the careful use of a two-dimensional wall adjustment strategy for three-dimensional flows, provided that specific model cross-stream span and blockage restrictions are met. Specifically, large wake flows were investigated using sharp-edged circular disks located on the longitudinal centerline of the test section. Drag coefficient data were in good agreement with the literature for solid blockage ratios of 3% or less, in contrast with the fixed wall test section limitation of 0.5% or less.[1] Additional testing constraints were found to be related to the unavoidable fixed side-wall pressure distortion, which limits the ratio of the model span to the width of the test section to 20% or less for an adaptive wall test section with a flexible roof and floor, compared with 10% for a fixed wall test section.[2]

This Note addresses and extends the useful spatial test envelope of the University of Waterloo Flexible Wall Wind Tunnel (UWFWWT).[3] The work confirms that three-dimensional models, such as a sphere, can be located asymmetrically to either side of the test section centerline and yet be satisfactorily examined using only the roof and floor centerline static pressure data and the unmodified two-dimensional wall adjustment strategy. The cross-stream distance c from the model center to the closer side wall is expressed as the model position ratio c/b, based on the overall test section width between the fixed side walls, b.

Overview of Experiments

Preliminary experiments[1] with an instrumented sphere model (127 mm in diameter) located on the test section centerline (Fig. 1) have shown that flowfield symmetry can be maintained under conditions of two-dimensional wall adaptation, provided that the model meets the span and blockage restrictions obtained in the disk studies. Further experiments were then conducted to investigate the onset of flowfield asymmetry as the sphere was located away from the test section centerline (toward one of the fixed test section side walls), under straight wall and adapted roof and floor conditions.

The sphere model was tested at a Reynolds number of $Re_d = 1.69 \times 10^5$ in the UWFWWT. Cross-stream measurement locations included the test section centerline, corresponding to $c/b = 0.5$, and near the fixed test section side wall, at $c/b = 0.2$. Intermediate positions of $c/b = 0.4$ and 0.3 were tested, but only under the influence of a straight roof and floor. Adapted wall solutions were computed using the two-dimensional predictive wall adjustment strategy of Wolf and Goodyer,[4] based solely on test section roof and floor centerline static pressure distributions. No laterally positioned roof or floor static pressure measurements were acquired regardless of the model's lateral position.

The experiment configuration represented a nominal solid blockage ratio of 3.6% and a model diameter-to-test-section-span ratio of 21%. These two parameters were within the three-dimensional model test constraints previously determined for models of bluff-body configuration.[2]

Measurements of the mean surface static pressure distribution $C_p(\theta)$ were acquired from 17 pressure taps on each side of the sphere (Fig. 1), defined by angular position θ (where $\theta = 0$ deg corresponds to the stagnation point). Surface static pressure information from $-160 \leq \theta \leq 165$ deg was compiled at roll angles of $\phi = 0, \pm 45$, and ± 90 deg (where $\phi = 0$ deg corresponds to vertical orientation of the static pressure taps and $\phi = +90$ deg is the horizontal orientation toward the side wall). The total drag coefficient C_D was obtained from a six-component sting force balance (Fig. 1).

Flow Symmetry Results Under Straight Walls

Under the influence of straight walls with the sphere located on the test section centerline ($c/b = 0.5$), $C_p(\theta)$ measurements were found to be independent of the roll angle, indicating a symmetric flow pattern about the sphere. Flowfield symmetry was maintained at $c/b = 0.4$. The surface pressure distribution noticeably departed from symmetry only for $c/b \leq 0.3$. In contrast, C_D measurements were found to be entirely independent of cross-stream position for $0.2 \leq c/b \leq 0.5$ and, by mirror image, to $c/b \leq 0.8$ (Table 1).

Flow Symmetry Results Under Adapted Walls

Two independent adapted wall solutions were obtained for $c/b = 0.5$ and one for each of the cross-stream positions $c/b = 0.4$, 0.3, and 0.2. For $c/b = 0.5$, the symmetrical flow pattern about the sphere was retained under adapted wall conditions, although the magnitude of the pressure distributions changed to reflect the minimization of wall interference effects, primarily through a correction to the base pressure (Fig. 2). This change was also reflected in a decrease in C_D (Table 1). The adapted wall results were confirmation of earlier work[1] and were consistent with previously published experimental work, such as that of Achenbach.[5] The favorable agreement with Achenbach's data also indicated that the interference of the sting airfoil support (Fig. 1) was effectively compensated for by roof and floor adaptation. Furthermore, an assessment of two-dimensional wall interference, for the sphere at $c/b = 0.5$, determined that the residual axial velocity perturbation along the test section centerline was reduced to less than 0.25% of the freestream velocity.[1] This value may be considered to be within the tolerated range for a well-designed aerodynamic wind tunnel and to permit comparison of results with reported reliable data.[2]

With the sphere positioned near the test section side wall, at $c/b = 0.2$, two-dimensional wall adaptation still resulted in changes to both

Table 1 Drag coefficient data[a] (total combined uncertainty of $C_D + 0.02$) for the sphere at $Re_d = 1.69 \times 10^5$

c/b	Wall setting	C_D
0.5	Straight walls	0.58
0.4	Straight walls	0.58
0.3	Straight walls	0.57
0.2	Straight walls	0.58
0.5	Adapted walls	0.54
0.2	Adapted walls	0.53
Published data,[5]	Re_d from 1×10^5 to 2×10^5	0.51–0.53

[a]The data remain independent of the cross-stream position and do not reflect the asymmetrical nature of the flowfield.

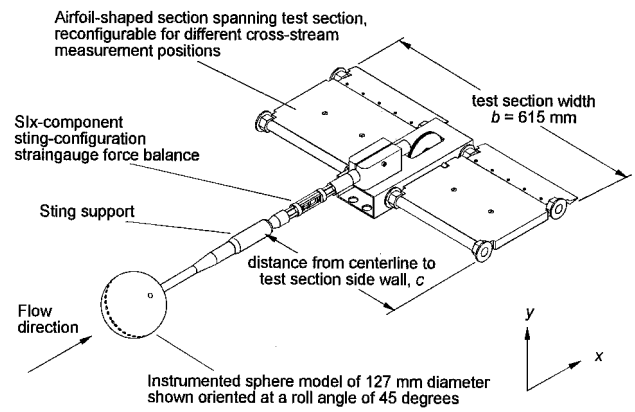

Fig. 1 Experiment configuration.

Received Oct. 8, 1996; revision received Jan. 24, 1997; accepted for publication Jan. 27, 1997.

*Graduate Student, Department of Mechanical Engineering; currently Graduate Student, Department of Mechanical Engineering, McGill University, 817 Sherbrooke Street West, Montréal, Québec H3A 2K6, Canada.
†Professor (retired), Department of Mechanical Engineering.

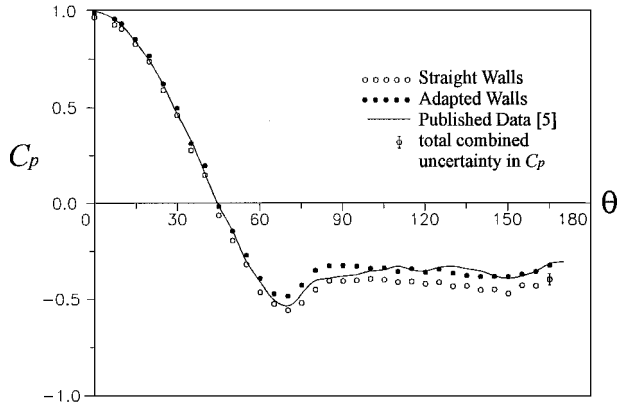

Fig. 2 Sphere surface static pressure distributions ($\phi = 0$ deg) with the sphere positioned on the test section centerline ($c/b = 0.5$), at $Re_d = 1.69 \times 10^5$, illustrating the effectiveness of the two-dimensional wall adaptation in removing the effects of wall interference. The total combined uncertainty is estimated at $C_p \pm 0.03$.

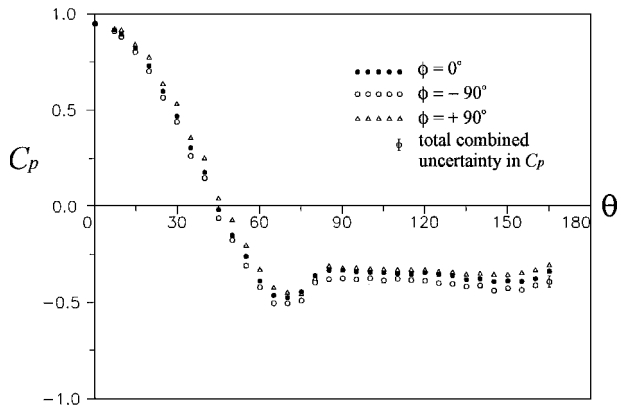

Fig. 3 Mean static pressure distributions at $c/b = 0.2$ and $Re_d = 1.69 \times 10^5$ for adapted walls. Two-dimensional wall adaptation provided a correction to the base pressure region but could not correct the asymmetrical nature of the flowfield about the sphere at this cross-stream position (total combined uncertainty of $C_p \pm 0.03$).

the $C_p(\theta)$ distribution and C_D (Table 1). The flow pattern, however, remained asymmetric (Fig 3).

Permissible Range for Cross-Stream Position

The permissible range for cross-stream position of the center of the sphere extends from the test section longitudinal centerline to a distance of $0.2b$ (121.9 mm) toward either side wall. Since the sphere has a radius of 63.5 mm ($0.10b$), the permissible range for model lateral position extends $\pm 0.3b$ from the centerline. Since a similar extension of the permissible working zone can also be accommodated in the vertical direction, through adjustment of the roof and floor contours,[3] a conservative estimate is placed on the permissible zone in which three-dimensional models such as a sphere can be located: it is assumed that the model must be located within a circle of radius $0.3b$, centered on the test section centerline. Thus the permissible test zone in which a sphere of 3.6% solid blockage can be placed is the central 28% of the test section cross-sectional area.

Conclusions

The experimental results lend further support to the careful use of a two-dimensional wall adjustment strategy for low-speed, three-dimensional flows under specific conditions for solid blockage of less than 4% for semiaerodynamic shapes, model span in the cross-stream direction of up to 20%, and model proximity to the side walls of $c/b \geq 0.3$. This result yields a permissible test zone comprising 28% of the test section area. The experiments also demonstrate that three-dimensional models such as a sphere can be tested in an environment of minimum wall interference without the need to employ a more computationally intensive and instrumentation-demanding three-dimensional wall adjustment strategy.

References

[1] Sumner, D., "An Experimental Investigation of Three-Dimensional Models in a Two-Dimensional Adaptive Wall Test Section," M.A.Sc. Thesis, Dept. of Mechanical Engineering, Univ. of Waterloo, ON, Canada, 1994.

[2] Sumner, D., and Brundrett, E., "Testing Three-Dimensional Bluff-Body Models in a Low-Speed Two-Dimensional Adaptive Wall Test Section," *Journal of Fluids Engineering*, Vol. 117, 1995, pp. 546–551.

[3] Kankainen, P., Brundrett, E., and Kaiser, J. A., "A Small Wind Tunnel Significantly Improved by a Multi-Purpose, Two-Flexible-Wall Test Section," *Journal of Fluids Engineering*, Vol. 116, 1994, pp. 419–423.

[4] Wolf, S. W. D., and Goodyer, M. J., "Predictive Wall Adjustment Strategy for Two-Dimensional Flexible Walled Adaptive Wind Tunnel—A Detailed Description of the First One-Step Method," NASA CR 181635, 1988.

[5] Achenbach, E., "Experiments on the Flow Past Spheres at Very High Reynolds Numbers," *Journal of Fluid Mechanics*, Vol. 54, Pt. 3, 1972, pp. 565–575.

R. W. Wlezien
Associate Editor

Near-Field Experiments on Tip Vortices at Mach 3.1

Frank Y. Wang* and Pasquale M. Sforza†
Polytechnic University, Brooklyn, New York 11201

Introduction

LIMITED experimental investigations of the supersonic flowfield behind low aspect ratio, unswept wings were conducted over four decades ago by Davis[1] and Adamson and Boatright.[2] Recently, pitot measurements of supersonic tip vortices from different unswept wings were made by Kalkhoran et al.,[3] Wang and Sforza,[4] and Wang.[5] Most recently, Smart et al.[6] made additional measurements in such flows using pitot and cone probes. This limited database prompted the present Note, which expands upon the key features of the previous findings. The tip vortex generator used is a straight half-wing with a modified double wedge airfoil and a 45-deg chamfer at the tip. It has a chord of 76.2 mm, a thickness of 7.9 mm, a span of 118.75 mm, and a half-wedge angle of 8.3 deg. The tests were made in a Mach 3.1 stream (25.4 × 26.2 cm tunnel cross section) at a Reynolds number of 7.08×10^6 based on the chord for two angles of attack.

Results and Discussion

Previous experience indicates that the diameter of the vortex core (defined as the distance between the swirl velocity peaks) is well represented by the size of the darker band trailing off the wingtip in shadowgraphs.[5] Core diameters, thus, were measured off shadowgraphs taken during the study,[4,5] resulting in values of 6.4 ± 0.8 and 8.5 ± 0.8 mm for $\alpha = 5$ and 10 deg, respectively. These shadowgraphs show virtually no change in the size of the core within the near-field viewing area. This suggests that the radial velocity component is small compared to the axial component and the effect of diffusion is minor, analogous to features found in the incompressible counterpart. Vortex locations were determined using a traversable pitot rake positioned horizontally across the tunnel centerline. Pitot pressure measurements (uncertainty of ± 1.86 kPa) were made at 2.3 chords downstream of the trailing edge for $\alpha = 5$ and 10 deg. This survey location was well within the region free of reflections of the wing's shock-expansion patterns. Pitot pressure results were

Received May 28, 1996; revision received Dec. 6, 1996; accepted for publication Jan. 28, 1997.

*Research Engineer, Department of Mechanical, Aerospace, and Manufacturing Engineering; currently National Science Foundation International Fellow, von Kármán Institute for Fluid Dynamics, 72 Chaussée de Waterloo, B-1640 Rhode-St-Genèse, Belgium. Member AIAA.

†Professor, Department of Mechanical, Aerospace and Manufacturing Engineering. Associate Fellow AIAA.